



Selective Catalytic Reduction on Filter Performance Testing on Non-road Diesel Engine

Kirsi Spoofo-Tuomi, Seppo Niemi, Teemu Ovaska, Olav Nilsson, and Sonja Heikkilä University of Vaasa

Krister Ekman Turku University of Applied Sciences

Citation: Spoofo-Tuomi, K., Niemi, S., Ovaska, T., Nilsson, O. et al., "Selective Catalytic Reduction on Filter Performance Testing on Non-road Diesel Engine," SAE Technical Paper 2021-01-5054, 2021, doi:10.4271/2021-01-5054.

Abstract

High-efficiency lean-burn compression ignition engines are expected to continue to play an important role as a power source for non-road mobile machinery. The challenge for these engines is that they suffer both high levels of nitrogen oxide (NO_x) and particulate matter (PM) emissions, and the simultaneous reduction of these particular emissions is difficult due to the trade-off relationship between NO_x and PM. Consequently, achieving the most stringent emission limits requires efficient exhaust aftertreatment. Traditionally, NO_x and PM have been controlled by separate aftertreatment devices. However, such sequential system configurations have several disadvantages, such as a large volume of the aftertreatment system. The compact design of a selective catalytic reduction (SCR)-coated diesel particulate filters (DPF), referred to as selective catalytic reduction on filter (FSCR), allows the reduction in aftertreatment system volume and mass. Another advantage is that the SCR can be placed closer to the engine to improve SCR temperature behavior. The major challenge of

the FSCR technology is the interaction between the SCR and DPF functions. The present study examines the operation of a state-of-the-art combined particulate filter and SCR catalyst device as a part of an exhaust aftertreatment system on a high-speed non-road diesel engine. Unlike previous studies, the goal was a complete ammonia (NH_3) slip-free operation. The main objective was to investigate how the SCR properties— NO_x conversion and NH_3 slip—change when the filter fills up with soot. In this context, tests with clean FSCR and with soot-loaded FSCR were conducted at varying urea dosing. The soot-loaded FSCR, compared with a clean one, showed a slightly (4-6%) lower NO_x reduction and higher (1-4 ppm) NH_3 slip under identical operating conditions. The results also indicated a decrease in NH_3 storage capacity upon soot loading. Finally, a supplementary flow-through SCR catalyst was added downstream of the FSCR, and tests with FSCR only versus FSCR + SCR were performed. Adding the second SCR allowed for higher urea dosing without NH_3 slip and, consequently, higher (+23%) NO_x conversions.

Keywords

Selective catalytic reduction, Nitrogen oxides, Diesel emissions, NO_x reduction, Exhaust aftertreatment, SCR coating on filter

1. Introduction

Historically, internal combustion engines (ICE) have dominated the power production in non-road mobile machinery (NRMM) [1], and for the vast majority of NRMM, the dominant power source is a diesel engine [2]. Several studies also predict that high-efficiency lean-burn compression ignition engines continue to play a central role in mobile machinery [3, 4, 5, 6], at least as long as alternative solutions provide the same flexibility and usability. Because of this, there is still great interest in improving the performance of diesel engines in terms of efficiency and exhaust emissions [2]. In recent years, research and development has focused on advanced combustion strategies (e.g., homogenous charge compression ignition, reactivity controlled compression ignition) [7], advanced fuel injection systems [8, 9],

optimization of geometrical features of the combustion systems [5, 9], and exhaust gas recirculation [10].

The challenge for diesel engines is that they suffer both high levels of nitrogen oxide (NO_x) and particulate matter (PM) emissions [3]. The simultaneous reduction of these particular emissions is difficult due to the trade-off relationship between NO_x and PM; engine control strategies that lead to a reduction of NO_x emissions increase particulate emissions and vice versa [7]. In practice, meeting the current, stringent EU Stage V NO_x and particulate limits for mobile non-road machinery requires efficient exhaust aftertreatment.

The implementation of increasingly stringent emission standards has given a massive boost to the development of exhaust gas aftertreatment technologies for the removal of NO_x and PM from diesel exhaust [11]. Traditionally, NO_x and

PM have been controlled by separate aftertreatment devices [12]. Selective catalytic reduction (SCR) is widely considered the most efficient solution for controlling NO_x emissions from diesel engines [13], while diesel particulate filters (DPF) are an established technology for reducing particulate emissions [11].

Such sequential system configurations, however, have several disadvantages: (1) A large number of exhaust gas cleaning devices and, consequently, a large volume of the exhaust gas after-treatment system; (2) inadequate temperature for the SCR functions, especially during cold starts, when the DPF is placed upstream of the SCR; and (3) unfavorable conditions for passive DPF regeneration—lower temperature and lower NO_2 —if the SCR is placed in front of the particulate filter [14].

To solve these problems, there is a lot of interest in integrating the functions of particulate filtration and NO_x reduction into a single multifunctional unit. One way to do this is to coat the highly porous walls of the DPF with SCR catalytic material [11, 12]. A compact design of an SCR-coated DPF, referred to as selective catalytic reduction on filter (FSCR) hereinafter, enables a reduction in aftertreatment volume and mass, closer placement of the SCR to the engine and faster light-off, improved heat transfer for soot conversion, and possible cost savings [14, 15].

One of the challenges of FSCR technology is the interaction between the SCR and DPF functions, i.e., the competition of nitrogen dioxide (NO_2) between NO_2 -assisted soot oxidation and NO_x reduction activities [12, 16, 17]. An additional challenge is the effect of soot loading on the mass diffusion from the exhaust stream to SCR catalytic sites and NO_x reduction [18].

The effect of soot loading on SCR reactions is debatably discussed in the literature. Watling et al. [12] reported that the presence of soot on the FSCR had no significant impact on NO_x conversion. Schrade et al. [19] performed steady-state NO_x conversion experiments with NO_2/NO_x ratios up to 0.5, showing that soot loading did not affect the SCR reactivity. With higher NO_2/NO_x ratios (>0.5), an increase in NO_x conversion efficiency was observed for soot-loaded FSCR. Similar results were reported by Tang et al. [17]. The authors concluded that the NO_2 reduction by soot oxidation results in higher NO_x conversions as the NO_2/NO_x ratio shifts towards the optimal point of 0.5 before reaching the SCR catalyst in the wall, promoting the Fast SCR reaction. Mihai et al. [20] found a slight decrease in NO_x conversion at 200–300°C in the presence of soot. This was explained by the blocking of the catalytically active sites. At higher temperatures, the NO_x conversion was slightly higher with soot, indicating that soot inhibited ammonia (NH_3) oxidation more strongly than the SCR reaction [20]. Also Marchitti et al. [21] reported a slight loss in the Standard and Fast SCR reactions (NO_2/NO_x ratio ≤ 0.5). Again, in the case of NO_2 excess ($\text{NO}_2/\text{NO}_x > 0.5$), an increase in NO_x conversion efficiency was observed for soot-loaded FSCR. To evaluate the influence of soot loading on the deNO_x behavior without interference of the soot/ NO_2 interaction as a possible side reaction, Purfürst et al. [22] investigated the catalytic deNO_x behavior of an FSCR in the Standard SCR reaction (NO_2/NO_x ratio = 0). They reported up to 20% lower NO conversion on a soot-loaded FSCR compared to a soot-free

FSCR. They concluded that the soot inside the porous filter wall acts as a diffusive barrier for the transport of gas species to the catalyst.

Another key parameter characterizing the performance of an FSCR is its NH_3 storage capacity, as the NO_x reduction efficiency depends on the amount of NH_3 stored on the catalyst [18]. In addition, a change in the NH_3 adsorption behavior will result in a changed NH_3 slip at the outlet of the SCR catalyst [22]. The effect of soot on NH_3 storage behavior is also controversially discussed in the literature. Schrade et al. [19] reported an increased NH_3 storage capacity of soot-loaded FSCR compared to the soot-free one. A maximum increase of 0.2 grams per liter (g/L) in NH_3 storage capacity was measured at 150°C. For higher temperatures, the soot effect was less pronounced. According to the authors, the measured effect was small, but it could affect the NH_3 slip in vehicle applications. Similar results were reported by Mihai et al. [20]. Elevated amounts of stored NH_3 indicated that some new NH_3 adsorption sites were created on the soot. Besides, a slightly higher release of unreacted NH_3 during the temperature ramp was observed in the presence of soot [20, 22]. Opposite conclusions were presented by Tan et al. [15], who found a decrease in the NH_3 storage capacity upon soot loading. For example, at 300°C, the PM loading reduced the NH_3 storage on the de-greened catalyst by approx. 0.25 g/L. For the aged catalyst, the effect of soot loading on NH_3 storage was negligible at temperatures above 250°C.

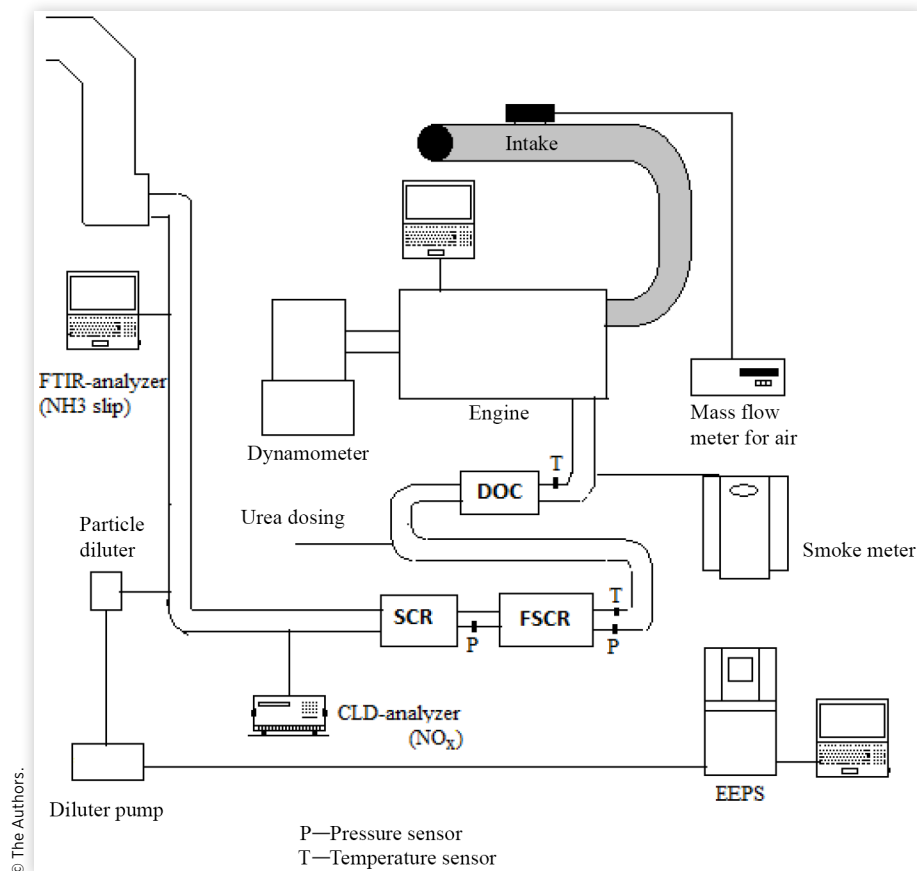
The objective of this study was to demonstrate the operation of a state-of-the-art combined particulate filter and SCR catalyst device as a part of an exhaust aftertreatment system. The engine experiments were performed by the University of Vaasa at the ICE laboratory of the Technobothnia laboratory unit. Before the investigation, the aftertreatment system was designed and matched with the 90 kW off-road diesel engine. The main aim was to investigate how the SCR properties— NO_x conversion and NH_3 slip—change when the filter fills up with soot. In this context, tests with clean FSCR and with soot-loaded FSCR were conducted at varying urea dosing. The goal was a complete NH_3 slip-free operation. Following this, a supplementary flow-through SCR catalyst was added downstream of the FSCR, and tests with FSCR only versus FSCR + SCR were performed. A diesel oxidation catalyst (DOC) was installed upstream of the FSCR to generate NO_2 for both the SCR reactions and soot oxidation.

2. Experimental Setup

The engine experiments were performed at the ICE laboratory of the University of Vaasa in Technobothnia laboratory unit in Vaasa, Finland. The experimental schema is illustrated in [Figure 1](#).

2.1. Research Equipment

The examined exhaust gas aftertreatment system was incorporated into the exhaust channel of a four-cylinder, common-rail diesel engine. The turbocharged, intercooled engine was

FIGURE 1 Experimental schema.

an AGCO Power 44AWI. The main specification of the test engine is given in [Table 1](#).

The aftertreatment system consisted of a bimetallic Pt-Pd oxidation catalyst (DOC) followed by urea injection and a silicon carbide wall-flow DPF coated with a copper (Cu)-zeolite-based SCR catalyst. The FSCR had a volume of 10.4 L. The cell density was 200 cells per square inch (cps). In the second phase of the experiments, a supplementary 6.4 L, 350 cps, flow-through SCR catalyst was added downstream of the FSCR. The metallic SCR substrate was also coated with a Cu-zeolite-based catalyst.

The canned catalyst elements were sized by the supplier. The sizing was based mainly on two constraints: the available space and the exhaust temperature range of the test engine.

TABLE 1 Test engine specification.

Engine	44AWI
Cylinder number	4
Bore (mm)	108
Stroke (mm)	120
Swept volume (dm ³)	4.4
Rated speed (rpm)	2100
Rated power (kW)	90
Maximum torque with rated speed (Nm)	410
Maximum torque with 1500 rpm (Nm)	525

The total exhaust aftertreatment system was placed on top of a horizontal level. The distances of the elements were kept as short as possible. On the other hand, the distance between the urea injection unit and the FSCR catalyst front edge was maximized in order to guarantee proper urea mixing. Therefore the exhaust pipe between the unit and the FSCR catalyst went beneath the level, and no urea mixer was needed. The catalyst elements and the pipes were insulated.

The engine was loaded by means of a Horiba eddy-current dynamometer WT 300. The sensor data were collected using software, made in the LabVIEW system-design platform. The primary quantities recorded were engine speed and torque, and the temperatures of cooling water, intake air, and exhaust gas. The pressures of intake air and exhaust gas were also followed with this data collection system. The engine control functions were monitored via a WinEEM4 program.

The emission measurement analyzers and instruments, adopted for the measurements, are presented in [Table 2](#). All measurements were performed downstream of the aftertreatment system.

2.2. Experimental Matrix

Emission measurements of clean and soot-loaded FSCR were performed at two constant engine operating points. The load points were the same as Points 2 and 3 of the 8-mode non-road steady cycle (NRSC) of the ISO 8178 standard. Tests with

TABLE 2 Emissions measurement analyzers and instruments.

For	Device	Technology
NO _x	Eco Physics CLD 822 M hr	Chemiluminescence
NH ₃	Gasmet DX4000	FTIR
Particle number and size distribution	TSI EEPS 3090	Spectrometer
Smoke	AVL 415 S	Optical filter
Air mass flow rate	ABB Sensyflow P	Thermal mass

© The Authors.

TABLE 3 Experimental matrix.

Point	2	3	7
Speed (rpm)	2100	2100	1500
Load (%)	75	50	50
Torque (Nm)	308	205	263

© The Authors.

FSCR only versus FSCR + SCR were conducted according to Point 7 of the NRSC. The speeds and loads are given in [Table 3](#).

At first, the engine was run without urea dosing. This way, the reference raw NO_x emissions were determined, to which the later NO_x values were compared.

Hereafter the appropriate urea injection quantities were searched, given as so-called alpha values. Alpha is the ratio of the injected urea amount and the theoretically required (stoichiometric) urea amount for complete NO_x removal. The stoichiometric urea dosing was calculated assuming 1:1 for NO_x:NH₃ stoichiometry and 1:2 for urea:NH₃ stoichiometry. The urea content of the injected AdBlue solution was 32.5%. Based on the difference between actual and target tailpipe NO_x, the theoretically required AdBlue dosing was determined as follows [23]:

$$\dot{m}_{\text{AdBlue,stoic}} = \frac{M_{\text{urea}}}{MF_{\text{AdBlue}}} \cdot \frac{SR_{\text{NO}_2}}{2 \cdot M_{\text{NO}_2}} \cdot \Delta \text{NO}_x = 2.008 \cdot \Delta \text{NO}_x$$

where $M_{\text{urea}} = 60.06$ g/mol, $M_{\text{NO}_2} = 46.0055$ g/mol, and AdBlue urea mass fraction $MF_{\text{AdBlue}} = 0.325$. SR_{NO_2} depends on the NO₂/NO_x ratio. $SR_{\text{NO}_2} = 1$, if NO₂/NO_x < 0.5 [23]. The stoichiometric AdBlue dosing quantity was calculated separately for each load point based on the raw NO_x concentration, as shown in [Table 4](#).

TABLE 4 Stoichiometric AdBlue dosing quantity for each load point.

Mode	Raw NO _x (ppm)	Raw NO _x (g/h)	Stoichiometric AdBlue quantity (g/h)	Stoichiometric AdBlue quantity (mg/s)
Clean FSCR; 2100 rpm/75% load	704	637	1279	355
Soot-loaded FSCR; 2100 rpm/75% load	668	607	1218	338
Clean FSCR; 2100 rpm/50% load	555	491	985	274
Soot-loaded FSCR; 2100 rpm/50% load	538	475	953	265
Clean FSCR; 1500 rpm/50% load	646	383	770	214
Clean FSCR + SCR; 1500 rpm/50% load	643	385	772	214
Soot loading; 1500 rpm/37% load	496	271	545	151

© The Authors.

In this study, the optimum alpha was determined as the urea dosing ratio, for which the most effective NO_x reduction is achieved without any NH₃ slip. To find the optimum alpha value, NO_x and NH₃ emissions were measured from the after-treated exhaust with different alpha ratios at each load point. The maximum NO_x conversion was reached by increasing the urea dosing quantity in ascending order. The urea dosage was increased until the NH₃ concentration in the exhaust exceeded 1 ppm, indicating NH₃ slippage. The optimum alpha value was defined as the urea-dosing ratio, for which the NH₃ concentration in the exhaust was less than 1 ppm. Prior to the measurements, the engine run was always stabilized, the criteria being that the NO_x concentration and temperatures of coolant water, intake air, and exhaust were stable.

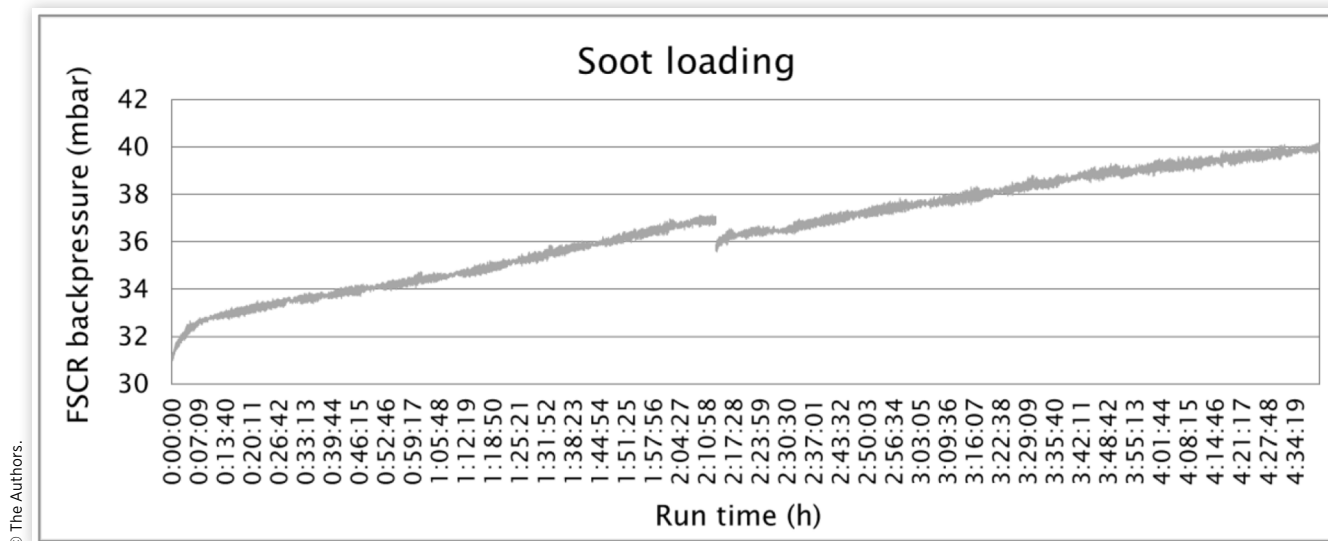
2.3. Soot Loading

The soot loading was performed by decreasing the engine fuel injection pressure to 40 MPa so that the Filter Smoke Number (FSN) measured by the AVL 415S smoke meter increased from 0.035 FSN to 0.35 FSN. The soot loading was continued until the backpressure level of 40 mbar was reached ([Figure 2](#)). During the loading, the engine was operated at an intermediate speed of 1500 rpm and 37% load. The exhaust gas temperature before the FSCR was of the order of 240°C. AdBlue dosing during soot loading was 30 mg/s, corresponding to an alpha ratio of 0.2. The loading was performed over two working days. Therefore there is a discontinuity in [Figure 2](#) at an FSCR backpressure of 37 mbar. The total running time during soot loading was 4 h 40 min.

The mass of trapped soot is most commonly expressed in grams per liter of filter. Many correlations have been developed that link FSN directly to soot mass emissions. Northtrop et al. [24] presented a comprehensive review of the topic. They found a strong correlation between the mass concentration calculated using the empirical correlation developed by Christian et al. [25] ([Equation 1](#)) and that measured from their experiments. The Christian correction method is also used in this study, resulting in a soot mass concentration of 4.886 mg/m³.

$$C = \frac{1}{0.405} \cdot 4.95 \cdot \text{FSN} \cdot e^{(0.38 \cdot \text{FSN})} \quad \text{Eq. (1)}$$

The measured exhaust mass flow rate was 344.9 kg/h, and the corresponding exhaust volume flow was 501 m³/h. As an

FIGURE 2 FSCR backpressure during soot loading.

© The Authors.

approximation, the properties of air were used for exhaust gas calculations. At 240°C, the exhaust gas density was determined to be 0.688 kg/m³, based on Equation 2.

$$\rho_{\text{air}} = \frac{p \cdot M_{\text{air}}}{R \cdot T} \quad \text{Eq. (2)}$$

The amount of trapped soot was then calculated by multiplying the exhaust gas volume flow by soot mass concentration and loading time. The total mass of soot accumulated on the walls of FSCR was 11.4 g. Dividing this by the filter volume gives the mass of trapped soot per liter of filter 1.1 g/L.

The maximum backpressure of the soot-loaded FSCR at a rated speed at 75% load was 76 mbar, and the maximum recommended exhaust backpressure for the engine was 200 mbar. Assuming an additional pressure drop of 100 mbar for the exhaust line piping and ducting [26], the soot mass load was well below the critical value.

3. Results and Discussion

This section presents the results of alpha tests with clean FSCR and with soot-loaded FSCR. The effect of soot on deNO_x performance is analyzed and discussed first and then followed by an analysis of the effect of soot on NH₃ slip. Finally, a supplementary flow-through SCR catalyst was added downstream of the FSCR, and the deNO_x performance and NH₃ slip behavior with FSCR only versus FSCR + SCR were analyzed.

3.1. Effect of Soot on DeNO_x Performance

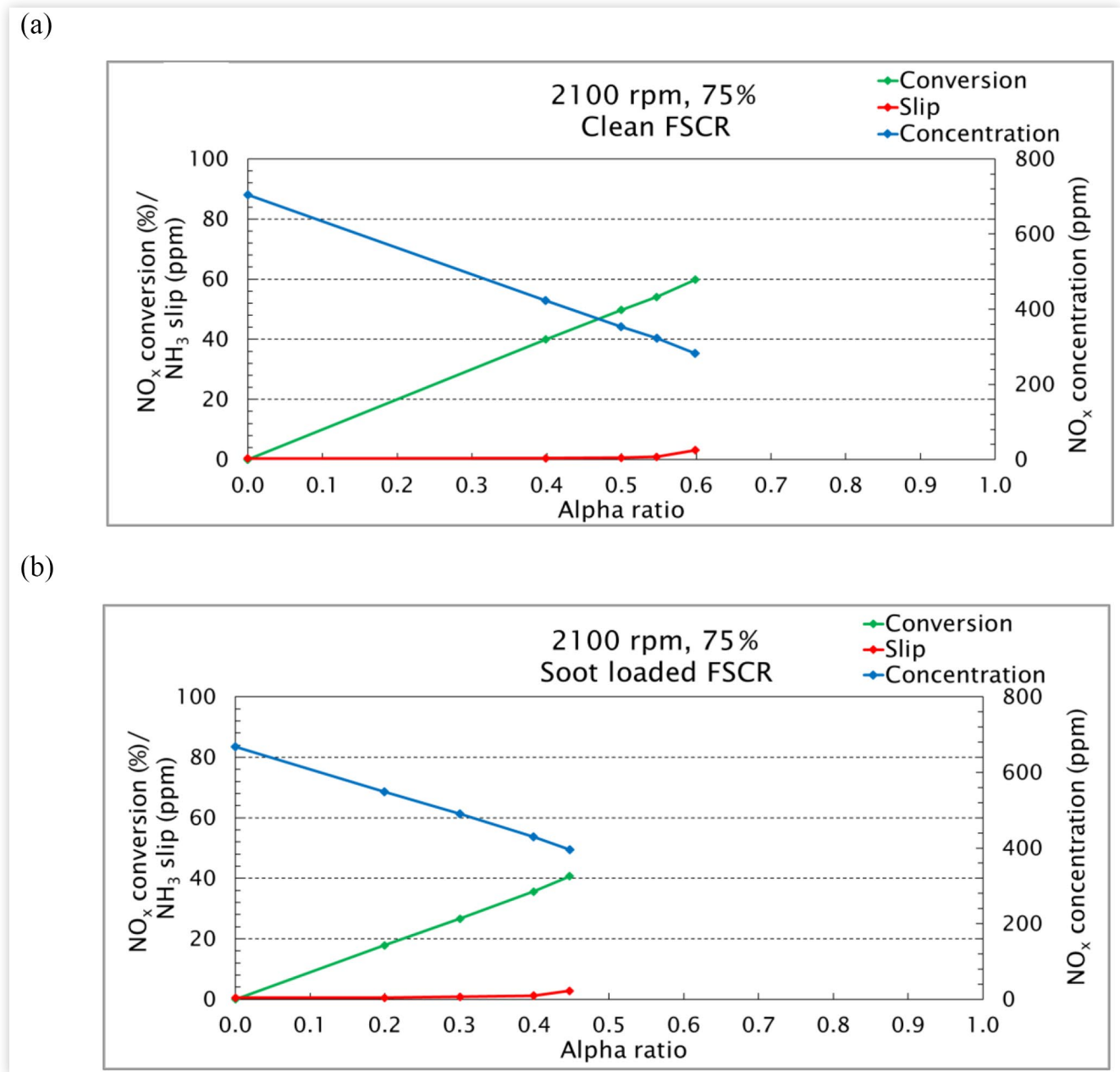
Figure 3 illustrates emission measurements of clean and soot-loaded FSCR at the rated speed at 75% load. Measurements were stopped when the NH₃ concentration of exhaust (red line) started to increase. The optimum alpha value was defined

as the urea-dosing ratio, for which the NH₃ slip was less than 1 ppm. The optimum alpha ratio for the clean FSCR was 0.55 and the corresponding NO_x conversion 54%. With soot-loaded FSCR, the NH₃ slip exceeded 1 ppm already with an alpha ratio of 0.4. Thus the optimum alpha was determined to be 0.3. The NO_x conversion at this point was 27%. The exhaust gas temperature was in the range of 326–334°C. When comparing the deNO_x performance under identical operating conditions, the NO_x conversion was slightly lower in the presence of soot. With an alpha ratio of 0.4, the NO_x conversion on soot-free FSCR was 40%, while on the soot-loaded FSCR the NO_x conversion was 36%.

At the rated speed at 50% load, the optimum alpha for the clean FSCR was 0.5 and the corresponding NO_x conversion 44% (Figure 4). With soot-loaded FSCR, the NH₃ slip started to increase right after the alpha ratio exceeded 0.2. Thus the optimum alpha was determined to be 0.2. The corresponding NO_x conversion was 19%. The exhaust gas temperature ranged from 246°C to 252°C. Again, NO_x conversion in identical operating conditions was slightly lower in the presence of soot. With an alpha ratio of 0.4, the NO_x conversion on soot-free FSCR was 37%, while on the soot-loaded FSCR the NO_x conversion was 31%.

A slight difference in the NO₂/NO_x ratio was detected in the feed gas. At 2100 rpm/75% load, the NO₂/NO_x ratio for the clean FSCR was 0.3 and for the soot-loaded FSCR 0.22. At 2100 rpm/50% load, the NO₂/NO_x ratio for the clean FSCR was 0.48 and for the soot-loaded one 0.41. Low NO₂/NO_x ratios are known to affect SCR performance by increasing the SCR dependency on Standard SCR reaction (Equation 3). As widely reported in the literature [21, 27, 28], higher NO_x conversions are achieved as the NO₂/NO_x ratio shifts towards the optimal point of 0.5, promoting the Fast SCR reaction (Equation 4).



FIGURE 3 NO_x concentration and conversion, and NH₃ slip at 75% load at 2100 rpm. (a) Clean FSCR, (b) Soot-loaded FSCR.

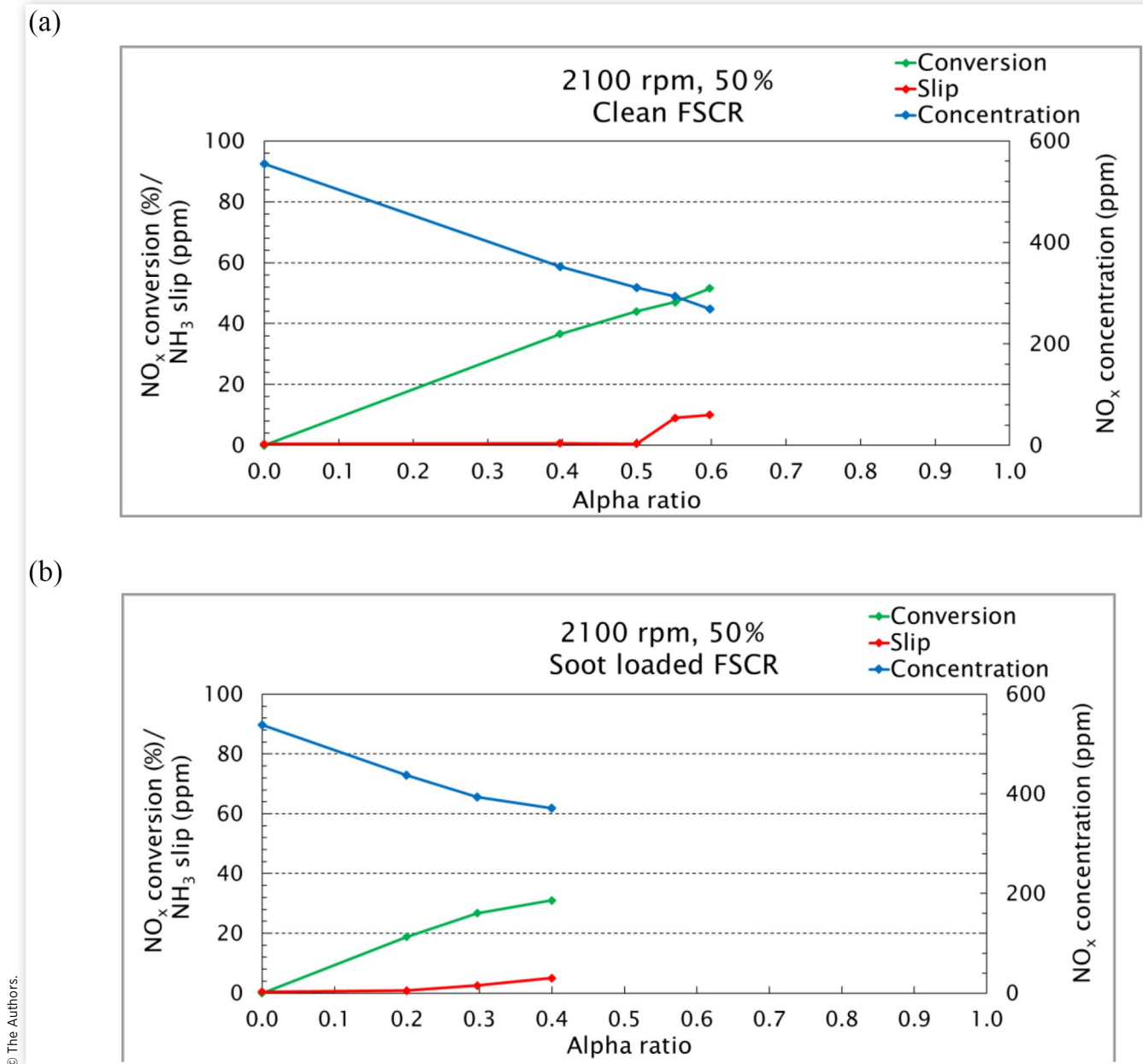
© The Authors.

However Cu-zeolite catalysts have been proven to have a low dependency on the NO₂ feed content [29, 30, 31]. For example, Kamasamudram et al. [31] reported that at steady state at 250-330°C, Cu-zeolite showed practically no loss of conversion using NO₂/NO_x feed ratios below 0.5.

Therefore the small difference in the NO₂/NO_x ratio was not considered to affect the results, and the slight decrease in NO_x conversions on soot-loaded FSCR was considered a physical rather than a chemical origin. Soot accumulation on the catalyst surface or active pore sites likely acted as a barrier inhibiting mass diffusion from gas flow to catalytic sites, as suggested by [16, 22, 32].

3.2. Effect of Soot on NH₃ Slip

Figure 5 brings into focus the change in the NH₃ slip behavior. An earlier NH₃ breakthrough in the presence of soot is observed, suggesting that soot limits the NH₃ adsorption rate. At 2100 rpm/75% load with an alpha ratio of 0.4, the NH₃ slippage on soot-free FSCR was 0.5 (±0.1); while on the soot-loaded FSCR, the NH₃ slip was 1.2 (±0.14). At 2100 rpm/50% load, the corresponding values were 0.7 (±0.1) for the clean FSCR and 5.0 (±0.5) for the soot-loaded one. The different occurrence of NH₃ slip under identical operating conditions

FIGURE 4 NO_x concentration and conversion, and NH_3 slip at 50% load at 2100 rpm. (a) Clean FSCR, (b) Soot-loaded FSCR.

© The Authors.

indicated that NH_3 emissions depend not only on the operating conditions but also on the deposits in the filter. This finding is well consistent with, e.g., Czerwinski et al. [13].

A slight decrease in NO_x conversion and an increase in NH_3 slip were also observed during soot loading. NO_x conversion and NH_3 slip as a function of FSCR backpressure during soot loading are presented in Figure 6.

3.3. FSCR + SCR Configuration

In the next phase, a supplementary flow-through SCR catalyst was added downstream of the FSCR, and alpha tests with FSCR only versus FSCR + SCR were done. Adding the second

SCR resulted in significantly higher alpha ratios and, thus, higher NO_x conversions, as seen in Figure 7. At the intermediate speed at 50% load, the optimum alpha for the FSCR was 0.6 and the corresponding NO_x conversion 55%. With the FSCR + SCR combination, the NH_3 slip exceeded 1 ppm with an alpha ratio of 0.9. The optimum alpha was thus determined to be 0.8. The NO_x conversion at this point was 78%. The exhaust gas temperature was in the range of 262–265°C. The NO_2/NO_x ratio was 0.4 in both cases. A more detailed representation of the NH_3 slip behavior of FSCR only versus FSCR + SCR combination is shown in Figure 8.

With this configuration, the FSCR can be placed closer to the engine, allowing for faster heat-up and earlier urea dosing during engine cold-start and warm-up situations, and consequently better NO_x control [13]. The downside is the

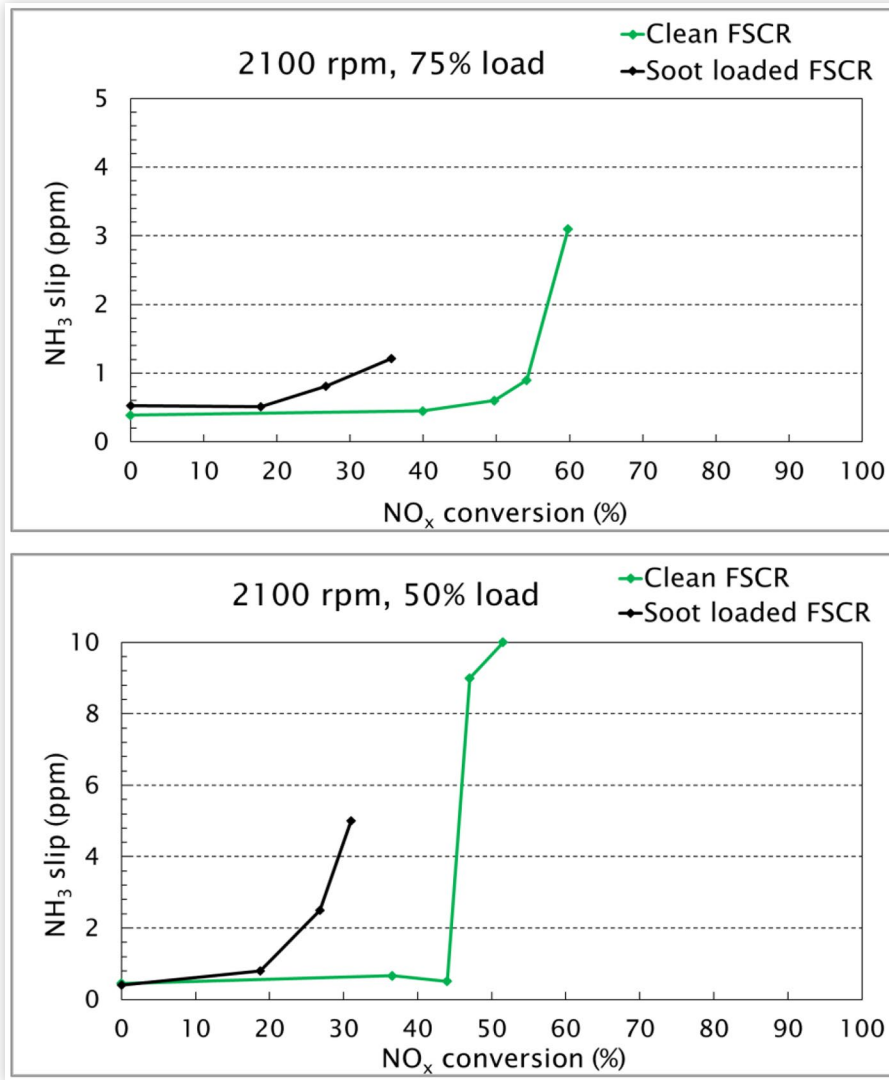
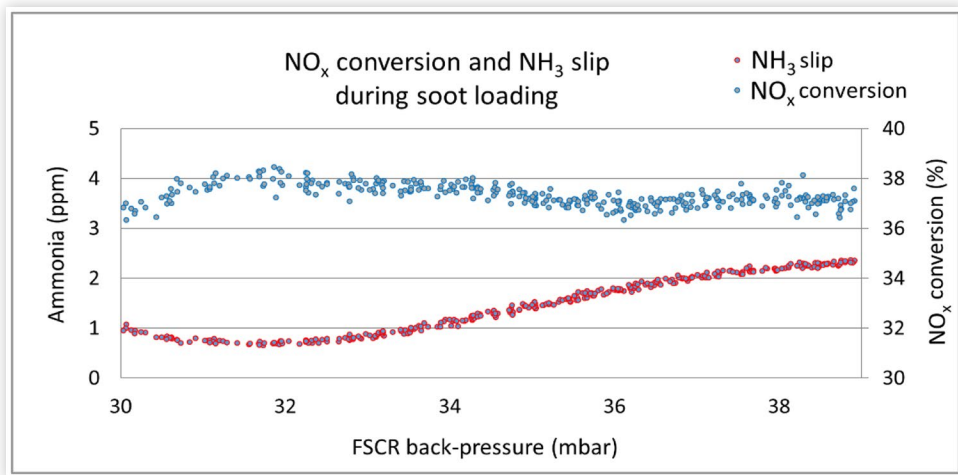
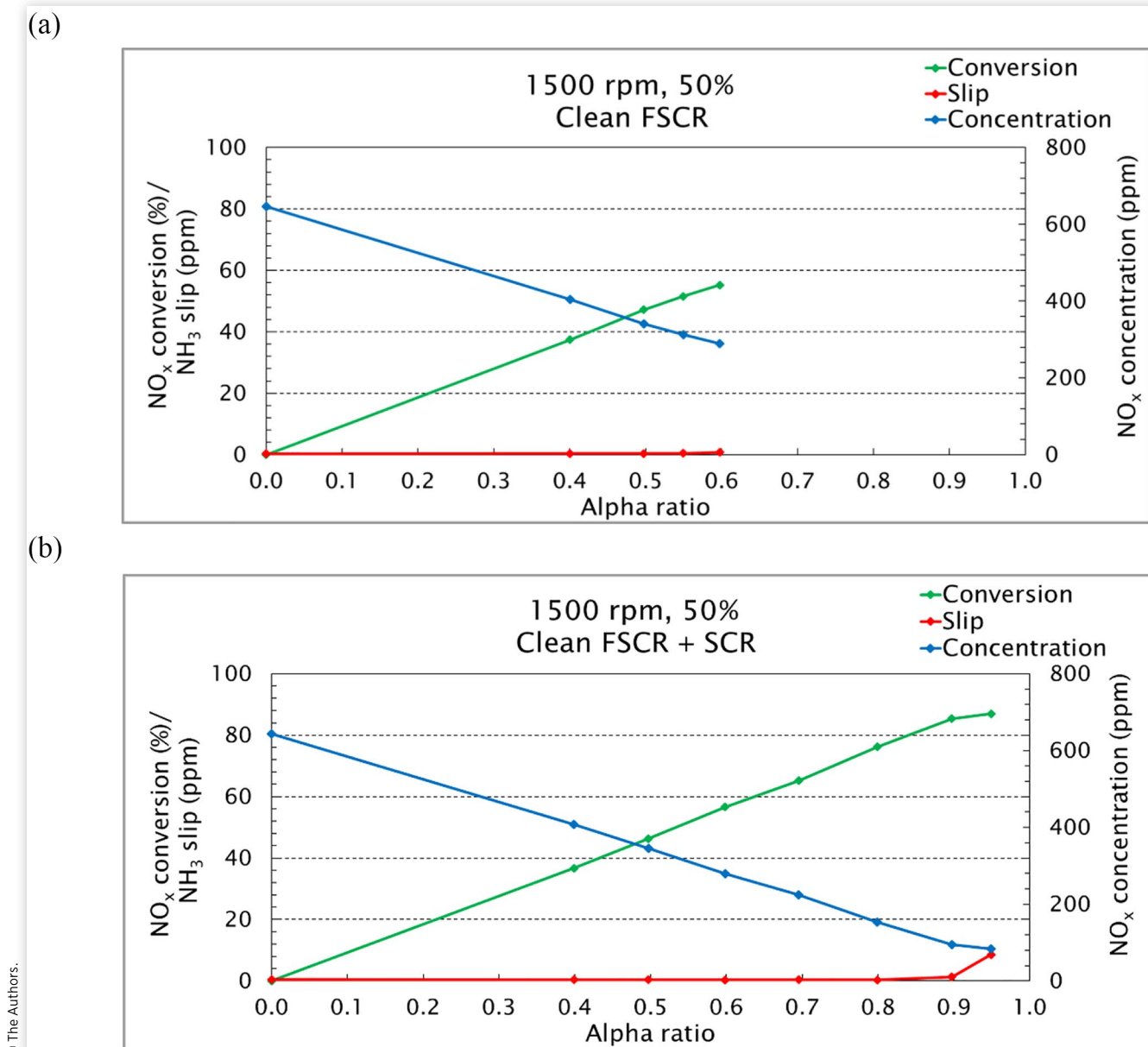
FIGURE 5 NH_3 slip at 75% and 50% load at 2100 rpm. Note different scales on the y-axis.**FIGURE 6** NO_x conversion and NH_3 slip as a function of FSCR backpressure during soot loading at 1500 rpm/37% load, AdBlue dosing 30 mg/s (alpha ratio of 0.2).

FIGURE 7 NO_x concentration and conversion, and NH_3 slip at 50% load at 1500 rpm. (a) Clean FSCR, (b) Clean FSCR + SCR.

© The Authors.

higher installation space requirement. Non-road applications often have limited space for aftertreatment installation.

Table 5 summarizes the maximum NO_x conversion rates obtained without NH_3 leakage ($\text{NH}_3 < 1$ ppm) and the corresponding alpha ratios, NH_3 concentrations, and exhaust gas temperatures upstream of the FSCR.

For future work, experimental studies on the impact of SCR reactions on soot combustion and passive filter regeneration are recommended.

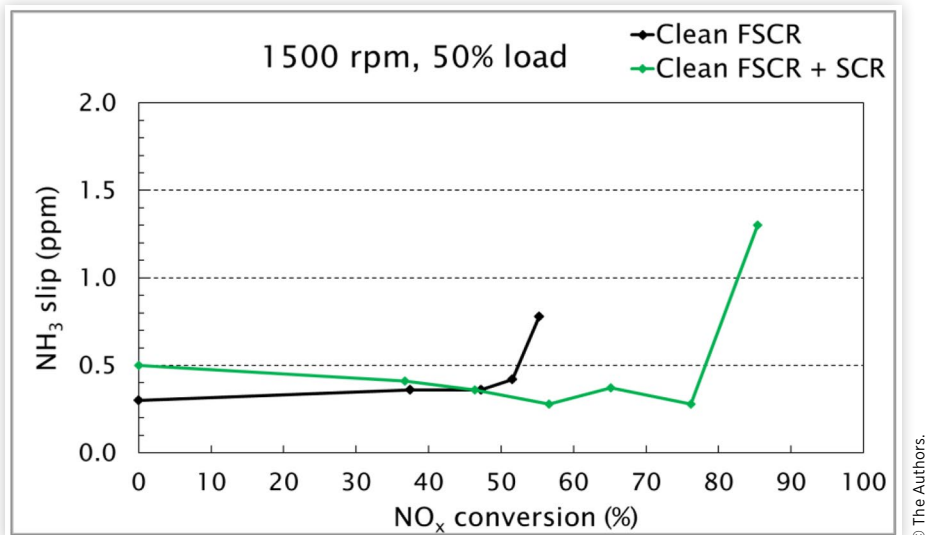
3.4. Particle Number and Size Distributions

Particulate sampling was conducted downstream of each exhaust aftertreatment configuration. The Engine Exhaust Particle Sizer (EEPS) signal was generally below its lower

detection limit, indicating high PN efficiency, but no other conclusions could be drawn from the results. To further examine, e.g., the effect of urea injection on the particulate number and size distribution, a lower dilution ratio must be applied for downstream FSCR measurements using EEPS.

4. Conclusions

The objective of this study was to demonstrate the operation of a state-of-the-art combined particulate filter and SCR catalyst device as a part of an exhaust aftertreatment system. The main aim was to investigate how the filter properties— NO_x conversion and NH_3 slip—change when the filter fills up with soot. Based on the engine experiments, the following conclusions were drawn:

FIGURE 8 NH₃ slip at 1500 rpm at 50% load: FSCR only versus FSCR + SCR combination.

© The Authors.

TABLE 5 NO_x conversions and NH₃ concentrations with optimum alpha values, and exhaust gas temperatures before the FSCR.

rpm/ load (%)	Clean FSCR				Soot-loaded FSCR				Clean FSCR + SCR			
	NO _x conv. (%)	Alpha ratio	NH ₃ slip (ppm)	Exh. temp. (°C)	NO _x conv. (%)	Alpha ratio	NH ₃ slip (ppm)	Exh. temp. (°C)	NO _x conv. (%)	Alpha ratio	NH ₃ slip (ppm)	Exh. temp. (°C)
2100/75	54	0.55	0.9	329	27	0.3	0.8	331	—	—	—	—
2100/50	44	0.5	0.5	246	19	0.2	0.8	252	—	—	—	—
1500/50	55	0.6	0.8	262	—	—	—	—	78	0.8	0.3	265

© The Authors.

- The soot-loaded FSCR, compared with a clean one, showed 4-6% lower NO_x reduction and 1-4 ppm higher NH₃ slip under identical operating conditions, i.e., at identical temperatures and alpha ratios.
- NO_x removal efficiency and NH₃ emissions depend not only on the operating conditions but also on the deposits in the filter.
- Adding the second SCR resulted in significantly higher alpha ratios and consequently higher NO_x conversions (+23%).
- For future work, experimental studies on the effect of urea injection on the particulate number and size distribution as well as on the impact of SCR reactions on soot combustion and passive filter regeneration are recommended.

Contact Information

Mrs. Kirsi Spoof-Tuomi
The University of Vaasa
PO Box 700, FI-65101 Vaasa, Finland
kirsi.spoof-tuomi@univaasa.fi

Acknowledgement

This study was funded from the European Union's Horizon 2020 research and innovation program under the grant agreement No 634135 (Hercules-2).

References

1. Lajunen, A., Sainio, P., Laurila, L., Pippuri-Mäkeläinen, J. et al., "Overview of Powertrain Electrification and Future Scenarios for Non-Road Mobile Machinery," *Energies* 11 (2018): 1184, doi:10.3390/en11051184.
2. Ratzinger, J.M., Buchberger, S., and Eichseder, H., "Electrified Powertrains for Wheel-Driven Non-road Mobile Machinery," *Automot. Engine Technol.*, 2020: 1-13, doi:10.1007/s41104-020-00072-z.
3. Leach, F., Kalghatgi, G., Stone, R., and Miles, P., "The Scope for Improving the Efficiency and Environmental Impact of Internal Combustion Engines," *Transportation Engineering* 1 (2020): 100005, doi:10.1016/j.treng.2020.100005.

4. Reitz, R.D., Ogawa, H., Payri, R., Fansler, T. et al., "The Future of the Internal Combustion Engine," *Int. J. Engine Res.* 21, no. 1 (2020): 3-10, doi:[10.1177/1468087419877990](https://doi.org/10.1177/1468087419877990).
5. Belgiorno, G., Boscolo, A., Dileo, G., Numidi, F. et al., "Experimental Study of Additive-Manufacturing-Enabled Innovative Diesel Combustion Bowl Features for Achieving Ultra-Low Emissions and High Efficiency," SAE Technical Paper 2020-37-0003, 2020, doi:<https://doi.org/10.4271/2020-37-0003>.
6. ERTRAC, "Future Light and Heavy Duty ICE Powertrain Technologies," ERTRAC Working Group Energy and Environment, April 5, 2016, https://www.ertrac.org/uploads/documents_publications/Roadmap/2016-04-05_ICE_roadmap_edited%20version.pdf.
7. Carder, D., Ryskamp, R., Besch, M., and Thiruvengadam, A., "Emissions Control Challenges for Compression Ignition Engines," *Procedia IUTAM* 20 (2017): 103-111, doi:[10.1016/j.piutam.2017.03.015](https://doi.org/10.1016/j.piutam.2017.03.015).
8. Di Blasio, G., Vassallo, A., Pesce, F., Beatrice, C. et al., "The Key Role of Advanced, Flexible Fuel Injection Systems to Match the Future CO₂ Targets in an Ultra-Light Mid-Size Diesel Engine," *SAE Int. J. Engines* 12, no. 2 (2019): 129-144, doi:<https://doi.org/10.4271/03-12-02-0010>.
9. Beatrice, C., Di Blasio, G., and Belgiorno, G., "Experimental Analysis of Functional Requirements to Exceed the 100kW/l in High-Speed Light-Duty Diesel Engines," *Fuel* 207 (2017): 591-601, doi:[10.1016/j.fuel.2017.06.112](https://doi.org/10.1016/j.fuel.2017.06.112).
10. Konstandopoulos, A.G., Kostoglou, M., Beatrice, C. et al., "Impact of Combination of EGR, SCR, and DPF Technologies for the Low-Emission Rail Diesel Engines," *Emiss. Control Sci. Technol.* 1 (2015): 213-225, doi:[10.1007/s40825-015-0020-0](https://doi.org/10.1007/s40825-015-0020-0).
11. Tronconi, E., Nova, I., Marchitti, F., Koltsakis, G. et al., "Interaction of NO_x Reduction and Soot Oxidation in a DPF with Cu-Zeolite SCR Coating," *Emiss. Control. Sci. Technol.* 1, no. 2 (2015): 134-151, doi:[10.1007/s40825-015-0014-y](https://doi.org/10.1007/s40825-015-0014-y).
12. Watling, T.C., Ravenscroft, M.R., and Avery, G., "Development, Validation and Application of a Model for an SCR Catalyst Coated Diesel Particulate Filter," *Catal Today* 188, no. 1 (2012): 32-41, doi:[10.1016/j.cattod.2012.02.007](https://doi.org/10.1016/j.cattod.2012.02.007).
13. Czerwinski, J., Zimmerli, Y., Mayer, A., D'Urbano, G. et al., "Emission Reduction with Diesel Particle Filter with SCR Coating (SDPF)," *Emiss. Control Sci. Technol.* 1 (2015): 152-166, doi:[10.1007/s40825-015-0018-7](https://doi.org/10.1007/s40825-015-0018-7).
14. Johansen, K., "Multi-Catalytic Soot Filtration in Automotive and Marine Applications," *Catal. Today* 258 (2015): 2-10, doi:[10.1016/j.cattod.2015.06.001](https://doi.org/10.1016/j.cattod.2015.06.001).
15. Tan, J., Solbrig, C., and Schmieg, S.J., "The Development of Advanced 2-Way SCR/DPF Systems to Meet Future Heavy-Duty Diesel Emissions," SAE Technical Paper 2011-01-1140, 2011, doi:<https://doi.org/10.4271/2011-01-1140>.
16. Colombo, M., Koltsakis, G., and Koutoufaris, I., "A Modeling Study of Soot and de-NO_x Reaction Phenomena in SCR/F Systems," SAE Technical Paper 2011-37-0031, 2011, doi:<https://doi.org/10.4271/2011-37-0031>.
17. Tang, W., Youngren, D., SantaMaria, M., and Kumar, S., "On-Engine Investigation of SCR on Filters (SCRoF) for HDD Passive Applications," *SAE Int. J. Engines* 6, no. 2 (2013): 862-872, doi:<https://doi.org/10.4271/2013-01-1066>.
18. Song, X., Johnson, J.H., and Naber, J.D., "A Review of the Literature of Selective Catalytic Reduction Catalysts Integrated into Diesel Particulate Filters," *Int. J. Engine Res.* 16, no. 6 (2015): 738-749, doi:[10.1177/1468087414545094](https://doi.org/10.1177/1468087414545094).
19. Schrade, F., Brammer, M., Schaeffner, J., Langeheinecke, K. et al., "Physico-Chemical Modeling of an Integrated SCR on DPF (SCR/DPF) System," *SAE Int. J. Engines* 5, no. 3 (2012): 958-974, doi:<https://doi.org/10.4271/2012-01-1083>.
20. Mihai, O., Tamm, S., Stenfeldt, M., Wang-Hansen, C. et al., "Evaluation of an Integrated Selective Catalytic Reduction-Coated Particulate Filter," *Ind. Eng. Chem. Res.* 54, no. 47 (2015): 11779-11791, doi:[10.1021/acs.iecr.5b02392](https://doi.org/10.1021/acs.iecr.5b02392).
21. Marchitti, M., Nova, I., and Tronconi, E., "Experimental Study of the Interaction between Soot Combustion and NH₃-SCR Reactivity over a Cu-Zeolite SDPF Catalyst," *Catal. Today* 267 (2016): 110-118, doi:[10.1016/j.cattod.2016.01.027](https://doi.org/10.1016/j.cattod.2016.01.027).
22. Purfürst, M., Naumov, S., Langeheinecke, K.-J., and Gläser, R., "Influence of Soot on Ammonia Adsorption and Catalytic DeNO_x-Properties of Diesel Particulate Filters Coated with SCR-Catalysts," *Chem. Eng. Sci.* 168 (2017): 423-436, doi:[10.1016/j.ces.2017.04.052](https://doi.org/10.1016/j.ces.2017.04.052).
23. Willems, F., "Modeling & Control of Diesel Aftertreatment Systems," TNO - TU/e - LiU Course 2015, https://www.fs.isy.liu.se/Edu/Courses/AftertreatmentMaC/Exercise_10_solution.pdf.
24. Northrop, W.F., Bohac, S.V., Chin, J.-Y., and Assanis, D.N., "Comparison of Filter Smoke Number and Elemental Carbon Mass From Partially Premixed Low Temperature Combustion in a Direct-Injection Diesel Engine," *J Eng Gas Turbine Power* 133, no. 10 (2011): 102804, doi:[10.1115/1.4002918](https://doi.org/10.1115/1.4002918).
25. Christian, V.R., Knopf, F., Jaschek, A., and Schindler, W., "Eine neue Messmethodik der Bosch-Zahl mit erhöhter Empfindlichkeit," *Motortech. Z.* 54, no. 1 (1993): 16-22.
26. Beatrice, C., Rispoli, N., Di Blasio, G., Patrianakos, G. et al., "Emission Reduction Technologies for the Future Low Emission Rail Diesel Engines: EGR vs SCR," SAE Technical Paper 2013-24-0087, 2013, doi:<https://doi.org/10.4271/2013-24-0087>.
27. Koebel, M., Madia, G., and Elsener, M., "Selective Catalytic Reduction of NO and NO₂ at Low Temperatures," *Catal. Today* 73, no. 3-4 (2002): 239-247, doi:[10.1016/S0920-5861\(02\)00006-8](https://doi.org/10.1016/S0920-5861(02)00006-8).
28. Rappé, K.G., "Integrated Selective Catalytic Reduction-Diesel Particulate Filter Aftertreatment: Insights into Pressure Drop, NO_x Conversion, and Passive Soot Oxidation Behavior," *Ind. Eng. Chem.* 53, no. 45 (2014): 17547-17557, doi:[10.1021/ie502832f](https://doi.org/10.1021/ie502832f).
29. Colombo, M., Nova, I., and Tronconi, E., "A Comparative Study of the NH₃-SCR Reactions over a Cu-Zeolite and a

- Fe-Zeolite Catalyst,” *Catal. Today* 151, no. 3-4 (2010): 223-230, doi:[10.1016/j.cattod.2010.01.010](https://doi.org/10.1016/j.cattod.2010.01.010).
30. Maunula, T., and Wolff, T., “Durable Copper and Iron SCR catalysts for Mobile Diesel and Dual-Fuel Applications,” SAE Technical Paper [2016-01-2214](https://doi.org/10.4271/2016-01-2214), 2016, doi:<https://doi.org/10.4271/2016-01-2214>.
31. Kamasamudram, K., Currier, N., Szailer, T., and Yezerets, A., “Why Cu- and Fe-Zeolite SCR Catalysts Behave Differently at Low Temperatures,” *SAE Int. J. Fuels Lubr.* 3, no. 1 (2010): 664-672, doi:<https://doi.org/10.4271/2010-01-1182>.
32. Park, S.-Y., Narayanaswamy, K., Schmiege, S.J., and Rutland, C.J., “A Model Development for Evaluating Soot-NO_x Interactions in a Blended 2-Way Diesel Particulate Filter/Selective Catalytic Reduction,” *Ind. Eng. Chem. Res.* 51 (2012): 15582-15592, doi:[10.1021/ie3020796](https://doi.org/10.1021/ie3020796).